Chlorinated benzenes and benzene degradation in aerobic pyrite suspension

Hoa Thi Pham[1]*, Inoue Chihiro[2]

[1]International University, Vietnam National University – Ho Chi Minh City
[2]Tohoku University

*Corresponding author's e-mail: phamhoa05@gmail.com

Abstract: The focus of this study is to investigate the applicability of natural mineral iron disulfide (pyrite) in degradation of aromatic compounds including benzene and several chlorinated benzenes (from mono-chlorinated benzene (CB), di-chlorinated benzenes (di-CBs) to tri-chlorobenzenes (tri-CBs) in aerobic pyrite suspension by using laboratory batch experiments at 25°C and room pressure. At first, chlorobenzene was studied as a model compound for all considered aromatic compounds. CB was degraded in aerobic pyrite suspension, transformed to several organic acids and finally to CO_2 and Cl^-. Transformations of remaining aromatic compounds were pursued by measuring their degradation rates and CO_2 and Cl^- released with time. Transformation kinetics was fitted to the pseudo-first-order reactions to calculate degradation rate constant of each compound. Degradation rates of the aromatic compounds were different depending on their chemical structures, specifically the number and position of chlorine substituents on the benzene ring in this study. Compounds with the highest number of chlorine substituent at *m*-positions have highest degradation rate (1,3,5-triCB > 1,3-diCB > others). Three chlorine substituents closed together (1,2,3-triCB) generated steric hindrance effects. Therefore 1,2,3-triCB wasthe least degraded compound The degradation rates of all compounds were in the following order: 1,3,5-triCB > 1,3-diCB > 1,2,4-triCB $\cong$ 1,2-diCB $\cong$ CB $\cong$ benzene > 1,4-diCB > 1,2,3-triCB. The final products of the transformations were CO_2 and Cl^-. Oxygen was the common oxidant for pyrite and aromatic compounds. The presence of aromatic compounds reduced the oxidation rate of pyrite, which reduced the amount of ferrous and sulfate ions release to aqueous solution.

Introduction

This study aims to investigate the degradation of benzene and chlorinated benzenes (from mono-, di- to tri-chlorobenzenes) in aerobic pyrite suspension. These compounds have been widely applied as intermediates and solvents in industry and agriculture. As a result of their universal use, they are nearly ubiquitous pollutants in air, water, sediments, and soils. They are on the priority list of hazardous substances published in 2017 by ATSDR, in which benzene is ranked at 6th; chlorobenzene (CB) at 128th; 1,2-dichlorobenzene (1,2-diCB) at 179nd; 1,3-dichlorobenzene (1,3-diCB) at 208rd; 1,4-dichlorobenzene (1,4-diCB) at 163th; 1,2,3-trichlorobenzene (1,2,3-triCB) at 137th; and 1,2,4-trichlorobenzene (1,2,4-triCB) at 202th position, out of a total of 275 hazardous compounds. They are chemically stable in both aerobic and anaerobic environments. For their acute toxicity and strong bioaccumulation potential, benzene and chlorobenzenes are of great health and environmental concern. Therefore, there is an urgent need to develop an effective control methods for this class of pollutants. There have been several techniques investigated for degradation of aromatic compounds, such as reduction zero-valent-iron with catalytic (Plagentz et al. 2006, Xu et al. 2005, Zhu et al. 2006),

electrochemical oxidation, oxidation by Fenton's reagent (Hsiao and Nobe 1993, Sedlak and Andren 1991), degradation by O_3/H_2O_2 (Ormad et al. 1997), or by photocatalytic (Zhang et al. 2007). However, there is still the need to develop a more cost-effective method through treatment techniques to minimize pollution.

Previous studies found the degradation of aliphatic chlorinated compounds, which were TCE and several aliphatic organic acids, in aerobic pyrite suspension (Pham et al. 2008, Pham et al. 2009, Che and Lee 2011). The hydroxyl radical induced from pyrite in aerobic solution is a very strong oxidant which can oxidize a variety of organic compounds (Ahlberg and Broo 1997, Berger et al. 1993, Borda et al. 2001, 2003, Cohn et al. 2004, 2005, 2006, 2008, Hao et al. 2006, Rimstidt and Vaughan 2003). There was very limited research on aromatic compounds, therefore, it is of interest to know whether the aromatic compounds also subjected to degradation reactions in pyrite aerobic suspension. In this study, the reactivity of pyrite toward degradation of aromatic compounds (including benzene and chlorinated benzenes) were conducted using lab scale batch experiments. The degradation reactions were pursued by measuring the disappearance of organic compounds and detecting the transformation products in the closed system.

Materials and methods

Materials

Standardaromatic compounds including 1,4-dichlorobenzene (1,4-diCB); 1,2,3 trichlorobenzene (1,2,3-triCB) and 1,3,5 trichlorobenzene (1,3,5-triCB) were bought from GL Sciences Inc., Japan. Benzene, chlorobenzene (CB), 1,2-dichlorobenzene (1,2-diCB), 1,3-dichlorobenzene (1,3-diCB) and 1,2,4-trichlorobenzene (1,2,4-triCB) in highest quality available were obtained from Wako Co., Japan. Benzene; CB; 1,2-diCB; 1,3-diCB and 1,2,4-triCB were used as the pure stocks without dilution. The remaining 3 compounds including 1,4-diCB; 1,2,3-triCB and 1,3,5-triCB were diluted in benzene solvent atthe concentration of 10 mg/ml. Standard organic acids including pyruvic acid, oxalic acid, acetic acid, and formic acid were bought in highest quality from Wako Co., Japan.

Massive natural mineral pyrite was received from Yanahara Mine in Okayama, Japan. The pyrite rock sample was ground with a ceramic mortar and pestle, further ground with a ceramic ball-mill and wet sieved. The fraction of 20 to 38 μm was retained for use. Scanning electron microscopy (SEM) and XRD analysis of the used pyrite mineral are shown to support information (Figure S.1 and Figure S.2). The morphology, elemental compositions and elemental mapping of unreacted pyrite are shown in Figure S.1. The surface of unreacted pyrite was partly oxidized (oxygen occupied about 7% (weight %) of mineral surface), and the surface contained minority amounts of Si (less than 0.4%). Peaks of Cu and Zn on the surface were invisible. The XRD diffractograms of unreacted pyrite show that all intense and well-defined peaks are attributable to pyrite (Figure S.2). All peaks are narrow showing the very strong crystallinity of the used pyrite mineral.

Prepared pyrite was rinsed several times with distilled water and ultrasonicated for 30 min to remove fine soil minerals from the surface. It was then dehydrated in a vacuum condition until used. After long storage, pyrite powder was washed again with 1 mol/L HCl solution to remove the oxidized layer on the surface. Washing the pyrite with the HCl solution did not affect its reactivity (data not shown). The metallic compositions of the used pyrite sample weremeasured by dissolving pyrite mineral in the HNO_3 solution and quantified using inductively coupled plasma mass spectrometry. Sulfur content was measured by combustion techniques coupled with precipitation as $BaSO_4$. Main elements included iron and sulfur at a molar ratio Fe:S of 1:1.85, which showedthat the pyrite was sulfur deficient. Si, Zn and Cu were presented as impurities. The molar percentages for S, Fe, Si, Zn, Cu, which were all the elements present, were 61.7, 33.3, 4.0, 0.7 and 0.2%, respectively. The specific surface area of the treated pyrite samples measured using the BETmethod was 0.2 m^2/g.

Experimental set up

The batch experiments were conducted in individual 26-mL glass vials. The vials contained 1g of pyrite and were filled with 10 ml of distilled water, leaving 16ml of head-space. Experiments were initiated by spiking the vials with a known concentration of the aromatic compounds, then crimp-sealed with Teflon-lined septa and aluminum cap and lastly wrapped by plastic wrapping in order to prevent any loss of the volatile organic compounds during the course of experiments. Each vial contained 100 g/L

FeS_2, resulting in the specific surface area concentration of 20 m^2/L. All vials had oxygen concentration initially in equivalent with the atmospheric air. At this condition, oxygen was found sufficient for the degradation of TCE and several organic acids (Pham et at., 2008). The prepared vials were placed on vortex shaker (TAITEC VR-36D) and shaken at 400 cycles/min in a temperature-controlled incubator (SANYO Electric Incubator MIR 153) at 25°C in dark in order to keep constant temperature and be isolated from any possible effect of light. Transformations of aromatic compounds were monitored for about 850 h. Control experiment or each treatment were concurrently performed under the same conditionsbut without pyrite added to assess any loss of aromatic compounds out of the vials and their absorbtion onto the vial glass wall and cap. All treatments were done in triplicate. At each sampling time, two ampules were removed from the incubator. The gas phase was injected into the gas chromatography (GCs) for analysis of organic compounds (CBs and benzene) and inorganic gases (CO_2, O_2). The ampule was then opened, filtered by 0.45 μm millipore membrane filter. The filtrate was collected for the purpose of measuring pH, ferrous, ferric ions, aqueous organic acids and inorganic ions (chloride and sulfate). Concentrations were quantified by comparison of GCs, HPLC or IC peak areas with the five-point standard curves. The change of pyrite mineral between before and after reacting with CB solution were characterization using XRD and SEM-XDS.

Analysis

Analyses of CBs and benzene were carried out with GC (GL Science Inc., GC-390) equipped with a flame ionized detector (GC-FID) and capillary column TC5 (GL Science Inc., 30 m in length, 0.32 mm inside diameter, and the film thickness 4 μm). GC parameters were optimized as injector temperature at 200°C; oven temperature at 120°C and detector temperature at 200°C;

Inorganic gases (CO_2, O_2) were analyzed using GC (GL Science, GC-323) equipped with thermal conductive detector (TCD) and capillary column (Porapak Q 50/80 column, GL Sciences). Thermal temperature was set at injection temperature at 120°C, oven temperature at 60°C and detector temperature at 100°C.

Chloride ion, sulfate ion and organic acids were measured using reversed phase ion chromatography IC (Metrohm, 761-Compact IC) equipped with Shodex SI-90 4E column, 1.7 mM $NaHCO_3$ and 1.8 mM Na_2CO_3 eluent, 1.0 ml/min flow rate, 25°C column temperature. Ferrous and ferric ions were measured by spectrophotometer at wavelength of 510 nm using phenonthroline method.

Pyrite surface morphology, elemental compositions and mapping were analyzed using scanning electron microscopy (SEM, Hitachi, Ltd.; S-4100) equipped with an energy--dispersive X-Ray spectrometer (EDS) detector (EDAX Genesis XM1- Ametek Inc., operating at 25 kV). Minerology of pyrite sample was measured by X-ray diffraction (XRD, Rigaku Corporation; CuKa=1.5406 A; 40 kV; 20 mA).

Results

Pyrite morphology and crystallinity analysis

The SEM micrographs presented in Fig. 1 shows the morphology of pyrite particles before and after reaction in CB solution. It can be seen that the surface layer of pyrite after reacting

with CB solution (Figure 1b) shows smoother and sharper edges compare to its initial condition (Figure 1a). Elemental compositions and elemental mapping of unreacted and reacted pyrite are shown in Figure S.1 and Figure 2. Theurface of both unreacted and reacted pyrite were partly oxidized (oxygen occupied about 7 weight % of mineral surface). Both surfaces contained minority amounts of Si (less than 2%). Peaks of Cu and Zn on both surfaces were invisible.

X-ray diffraction (XRD) patterns of unreacted and reacted pyrite in CB solution are displayed in Fig. 3. All intense and well-defined peaks are attributable to pyrite. The peaks of pyrite oxidation products were unrecognizable in both cases. The narrow peaks for both pyrites show very strong crystalinity of pyrite in both cases (half-value width B of all peaks varied in the range of 0.10 to 0.18). Table 1 shows the relative intensities of crystal planes of unreacted and reacted pyrite in comparison with standard pyrite. The main XRD peak of the used pyrite mineral, Yanahara mine pyrite with S:Fe = 1.85, is different fromthe standard pyrite mineral. This difference may be due to different type of pyrites. However, the XRD measurement of unreacted and reacted of the same pyrite mineral showed that the main peaks and the intensities of each XRD peaks were changed (Figure 3). Intensities of almost crystal planes of reacted pyrite decreased, except intensities of [210] and [311] planes increased compare with unreacted pyrite. It means that the rates of pyrite dissolution in CB solution are not the same for all planes. However, the crystal planes which were important for the degradation of organic compounds were unknown.
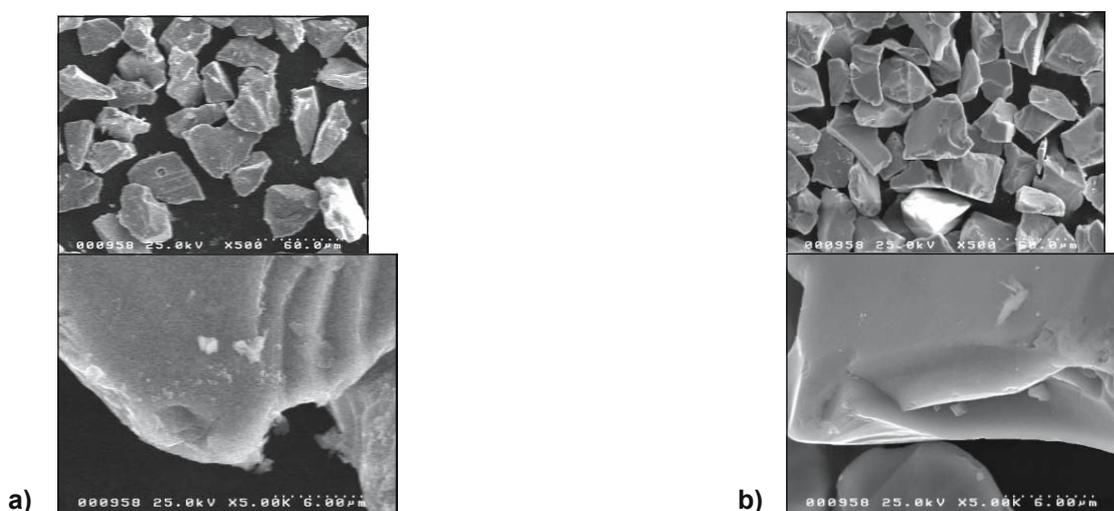
Fig.1. Secondary electron images of used pyrite mineral: (a) before experiment and (b) after 800h experiment with CB
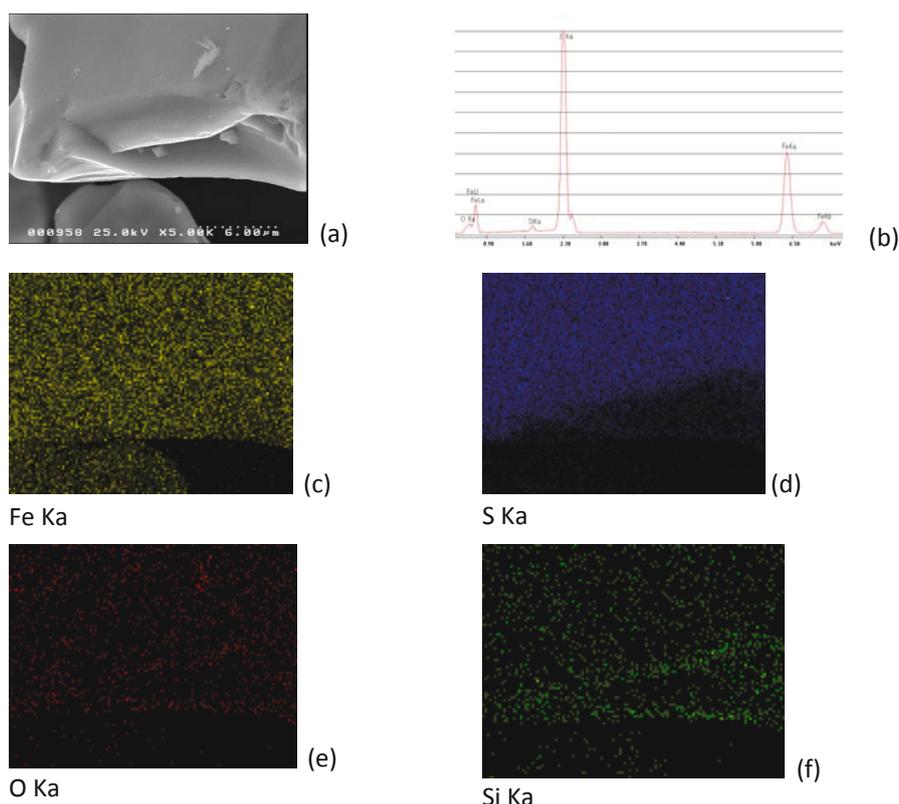
Fig. 2. SEM image and elemental mapping of reacted pyrite samples after 800 h reaction with CB

Upper left: SEM image of a composite reacted pyrite particle after 800 h in CB solution. Upper right: Elemental analysis shows clear peaks corresponding to Fe, O, S and 2.0 atomic % Si. Peaks of each element are shown on top of each peak.

CB degradation in aerobic pyrite suspension

At first, CB was investigated as a model compound for all aromatic compounds. CB degradation in aerobic pyrite suspension was monitored for 400h. Reaction solution had an initial pH of 4.0 and it was reduced to 2.9 at the end of the experimental course. Because no buffer was used to maintain constant pH, the pH of the solution was only controlled by oxidation reactions of pyrite and degradation reactions of organic compounds, which released protons to the solution. Figure 4 displays the disappearance of CB, the release of chloride to solution and the production of CO_2 into the gas phase with time. CB degraded by 80% of its initial concentration after 400 h. In response to CB disappearance, chloride ion and CO_2 concentrations both increased with time. Transformation kinetics of CB was fitted to pseudo-first-order reaction. The rate constant value was calculated from the linear regression of $\ln(C/C_i)$ vs. time, where C and C_i are the concentrations of TCE at time t and time zero, respectively. The observed pseudo-first-order rate constant for CB transformation was $3.6 \cdot 10^{-3}$ (h^{-1}).

Ratio of chloride and CO_2 with total degraded C were considered to assess the transformation pathways of CB degradation. Ratio of chloride and CO_2 were calculated following equations (1) and (2).

$$Ratio_{Cl^-} = C_{Cl^-} / (n_{Cl} \times \Delta C_{organicstransformed}) \qquad (1)$$

$$Ratio_{CO_2} = C_{CO_2} / (n_C \times \Delta C_{organicstransformed}) \qquad (2)$$

Where C_{Cl^-} and C_{CO_2} are concentration of Cl and CO_2; n_C and n_{Cl} are total number of C and Cl in organic compounds, $\Delta C_{organic\ transformed}$ is the concentration of organic compounds degraded. If $Ratio_{Cl^-}$ and $Ratio_{CO_2}$ equal to 1 mean that all degraded organic compounds transformed to CO_2, chloride and H^+. $Ratio_{Cl^-}$ and $Ratio_{CO_2}$ calculated from experimental data of CB show in Figure 4. The obtained $Ratio_{Cl^-}$ varied from 0.4 to 0.7, while $Ratio_{CO_2}$ was only in the range of 0.05 to 0.08. It means that the majority of CB transformed to organic compounds intermediates before finally degraded to CO_2. However, almost degraded Cl is in the form of chloride ion in solution. The transformation of CB to final products (CO_2 and chloride) is thermodynamically favorable (free Gibbs energy of -2971 kJ/mol) (Eq. 3).

$$C_5H_5Cl + 6O_2 \rightarrow Intermediates \rightarrow 5CO_2 + HCl + 2H_2O \quad (3)$$

Degradation intermediates and products, besides Cl^- and CO_2, were identified using reversed phase ion chromatography. The peaks of acetic acid and oxalic acid were identified, but the peaks of pyruvic acid and formic acid were overlapped under the analytical conditions (Figure 5). From this data set, it can be seen that CB effectively degraded in aerobic pyrite suspension. Before degradation to the final products as CO_2 and Cl^-, the
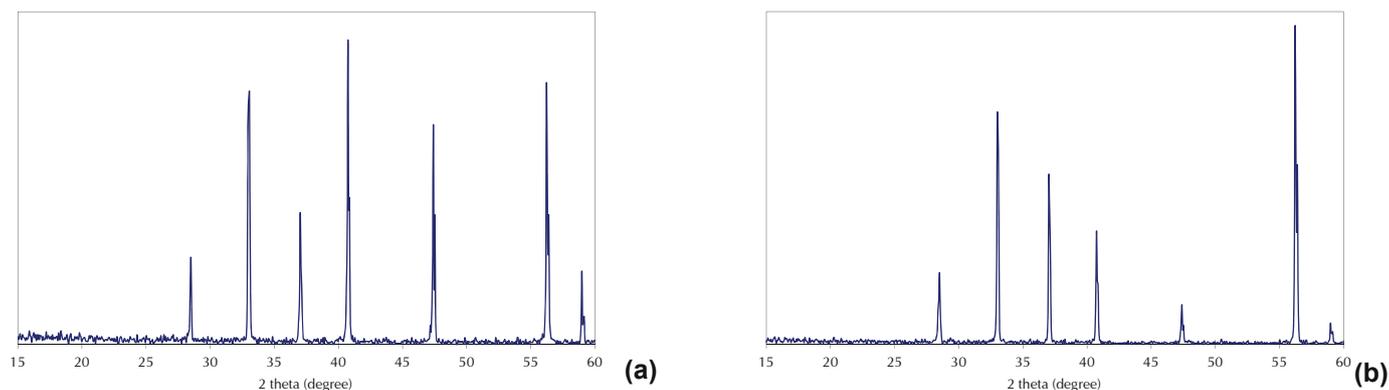
Fig. 3. XRD measurements of unreacted (above) and reacted pyrite (below)

Table 1. Relative intensities of crystal phases of unreacted and reacted pyrite in comparison with standard pyrite

hkl	2θ (degree)	d (Å)	I/Imax		
			unreacted pyrite	reacted pyrite	pyrite standard
[111]	28.50	3.128	27.1	20.1	31.0
[200]	33.06	2.705	82.6	72.7	100.0
[210]	37.02	2.420	42.6	52.2	53.0
[211]	40.74	2.210	100.0	35.3	40.0
[220]	47.4	1.916	72.2	11.8	36.0
[311]	56.22	1.633	84.9	100.0	69.0
[222]	58.98	1.563	23.7	6.3	11.0

main transformation pathways of this aromatic compound can be produced by several organics intermediates.

Benzene degradation in aerobic pyrite suspension

After CB degradation experiments, benzene degradation in pyrite aqueous solution was investigated. Benzene was known as a recalcitrant organic pollutant. However, it degraded in pyrite aqueous solution. Batch experiments were conducted using the same procedure as CB experiments and were monitored for 500 h. Figure 6 displays the disappearance of benzene and the production of CO_2 into the gas phase with time. Benzene degraded 80% of its initial concentration after 500 h.

In response to benzene disappearance, CO_2 concentrations increased with time. Transformation kinetics of benzene was fitted to pseudo-first-order reaction. The observed pseudo-first-order rate constant for benzene degradation was 3.7×10^{-3} (h^{-1}), which was equal to the degradation rate of CB. The amount of CO_2 produced only accounted for less than 10% of total degraded C, which was also similar to CB degradation. This fact means that the chlorine substituent on the benzene ring in CB does not affect the oxidation reaction of the benzene ring with hydroxyl radical. Further investigations on the transformation pathways of benzene and CB are necessary to understand degradation mechanism of aromatic compounds.
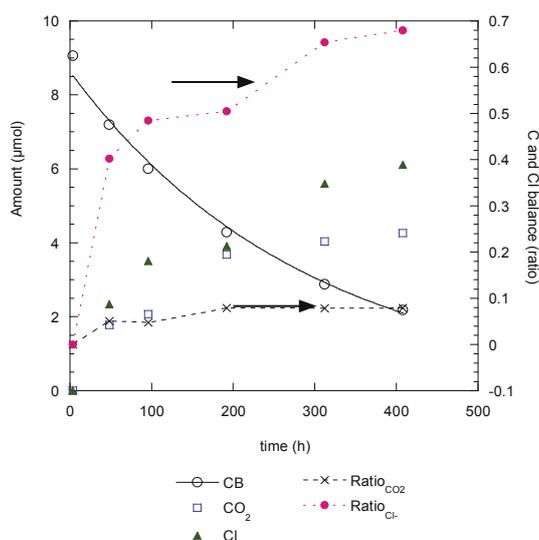
Fig. 4. Degradation of CB, production of chloride and CO_2, *Ratio*$_{Cl^-}$ and *Ratio*$_{CO_2}$ (pyrite suspension 20 m^2/L, 25°C, initial oxygen concentration in equivalent with atmospheric air)
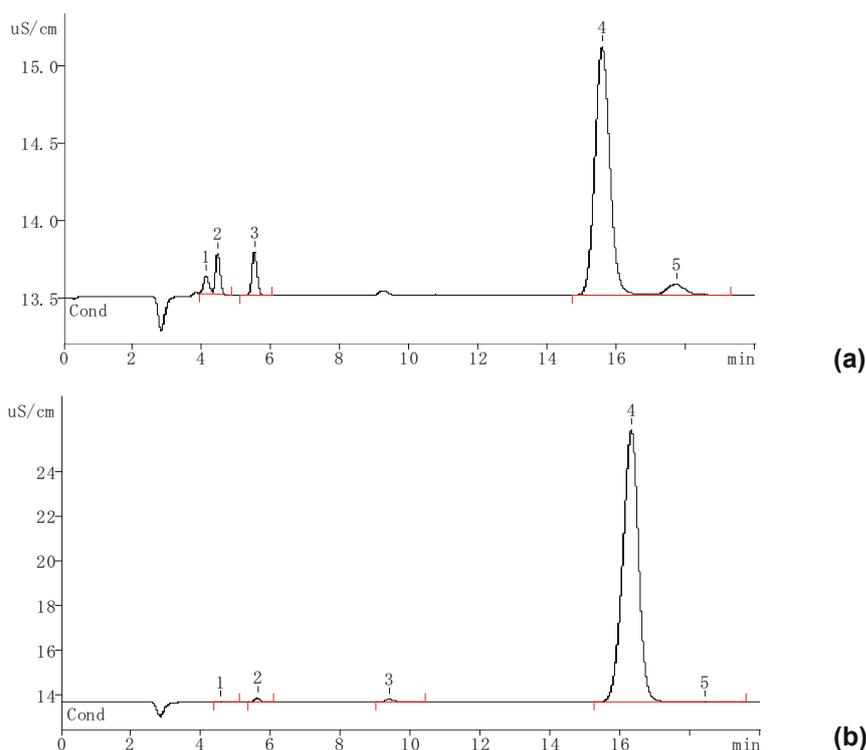
Fig. 5. Ion chromatography spectra. a) CB in pyrite suspension (Peak names: 1. Acetic acid, 2. Pyruvic acid and/or formic acid, 3. Chloride ion, 4. Sulfate ion, 5. Oxalic acid); b) Pyrite suspension blank (Peak name: 2. Chloride ion, 4. Sulfate ion)
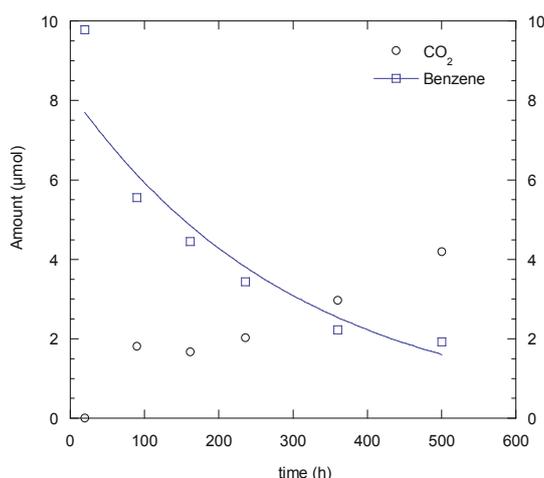
Fig. 6. Degradation profile of benzene and production of CO_2
(pyrite suspension 20 m²/L, 25°C, initial oxygen in equivalent with atmosphere)

Di- and tri-chlorinated benzenes degradation in aerobic pyrite suspension

After CB and benzene experiments, several higher chlorinated benzene including dichlorobenzenes (1,2-diCB; 1,3-diCB; and 1,4-diCB) and trichlorobenzenes (1,2,3-triCB; 1,3,5-triCB and 1,2,4-triCB) were investigated for the degradation in aerobic pyrite suspension. Batch experiments were conducted using the same procedure as CB experiments and were monitored for 850 h. The degradation profiles and CO_2 productions of all compounds are presented in Figure 7 and Figure 8. Within all investigated compounds, 1,3,5-triCB and 1,3-diCB degraded quickly within 100h. The two compounds including 1,2-diCB and 1,2,4-triCB were degraded at similar rates with CB and benzene, 80% of initial concentration disappeared within 500h. The remaining two compounds, which were 1,2,3-triCB and 1,4-diCB, were the most stable compounds under the experimental conditions.

In term of CO_2 production, in the experiments with 1,2-diCB; 1,3-diCB and 1,2,4-triCB (Fig. 7), pure stocks without dilution were used. As solvent was not used for the dilution of stock, therefore, there was only the transformation of investigated compounds that occurred in the vials. Generated CO_2 accounted for 8 to 20% of total degraded C. The majority parts of degraded C were in other forms of intermediates or products. In the experiments with 1,2,3-triCB; 1,3,5-triCB and 1,4-diCB (Fig. 8), the stocks diluted in benzene at concentration of 10mg/ml were used. Therefore, there was the transformation of the investigated compounds together with transformation of benzene occuring in the closed vials, as benzene was used as a solvent for dilution. The initial amount of benzene in these experiments was 56 µmol, while initial amounts of 1,2,3-triCB; 1,3,5-triCB and 1,4-diCB were 0.28, 0.28 and 0.34 µmol, respectively. The CO_2 productions in these experiments were mainly from benzene transformation.

Table 2 shows the calculated using equation (1) for all di- and tri-chlorobenzenes transformations in aerobic pyrite suspension. was obtained in the range of 0.7 to 1.1. It means that almost degraded chloride transformed to aqueous chloride ion. The chloride balance for 1,4-diCB and 1,2,3-triCB was a bit higher than 1 for two reasons, 1) the small initial concentrations and slow degradation of these compounds led to low concentration of chloride released to aqueous solution; 2) chloride was also released from dissolution reaction of pyrite due to the impurities in pyrite. Therefore analytical errors for these two compounds were higher than for other compounds.

Kinetics of all transformations was fitted to pseudo-first-order reactions. Degradation profiles of all aromatic compounds with time are shown in Figure 9. The apparent rate constants is shown in Table 3. Depending on the chemical structure, the rate constants obtained were different, ranging from 4.2×10^{-5} to 2.03×10^{-2} (h⁻¹). Transformation rates were different in the order of 1,3,5-triCB > 1,3-diCB > 1,2,4-triCB $\cong$ 1,2-diCB $\cong$ CB $\cong$ benzene > 1,4-diCB > 1,2,3-triCB. The difference in degradation rates of the aromatic compounds can be explained by the difference in the number and position of chlorine substituent on benzene ring. Chlorine substituent on the benzene ring directs the incoming substituent to ortho- and para-positions. When di- or tri-chlorine substituted benzenes undergo an electrophilic aromatic substitution, the directing effect of all substitutents has to be considered, together with the steric hinderance effect (Bruice 2004). If the directors direct the incoming substituent to the same positions, there are enhanced effects. It can be seen that 1,3,5-triCB has three *ortho* and *para* positions enhanced by three chlorines directors. 1,3-diCB has three *ortho* and *para* positions enhanced by two chlorines directors. Because of these directors, the higher degrees of oxidation are expected to be produced in oxidation of 1,3,5-triCB and 1,3-diCB compared to oxidations of other compounds. Therefore, degradation rates of 1,3,5-triCB and 1,3-diCB will be higher than of other compounds. In addition, between 1,3,5-triCB and 1,3-diCB, degradation rate of 1,3,5-triCB is higher than of 1,3-diCB. On the other hand, 1,2,3-triCB has three chloride atoms next to each other create the steric hindrance effect, therefore it is the more difficult to oxidize than other compounds. The degradation rate of 1,2,3-triCB is the smallest. The degradation rates of all compounds can be arranged in the following order: 1,3,5-triCB > 1,3-diCB >1,2,4-triCB $\cong$ 1,2-diCB $\cong$ CB $\cong$ benzene > 1,4-diCB > 1,2,3-triCB. CO_2 and Cl⁻ were the final products of all transformations.
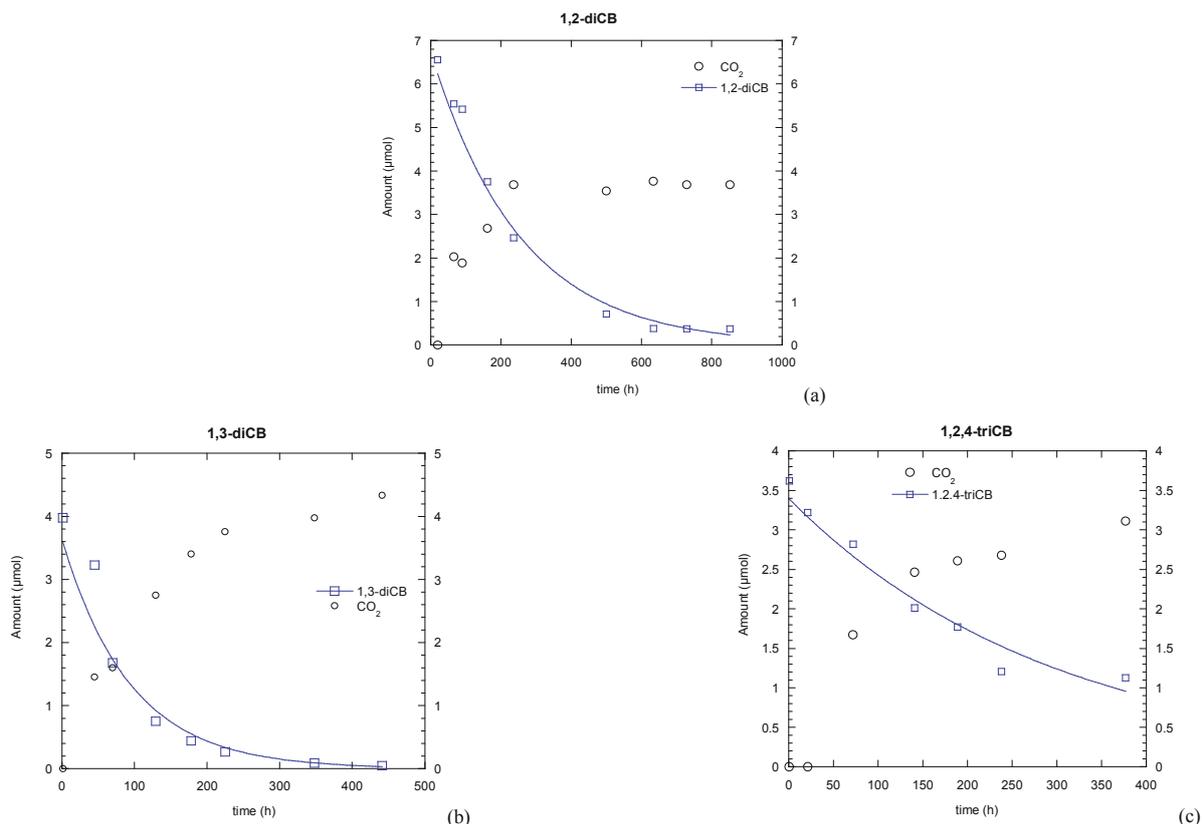
Fig. 7. Degradation profiles of aromatic compounds and CO_2 productions in pyrite suspension (20 m²/L), 25°C, initial oxygen in equivalent with atmosphere; a) 12-diCB; b) 13-diCB; c) 124-triCB; Pure stocks of all compounds were used
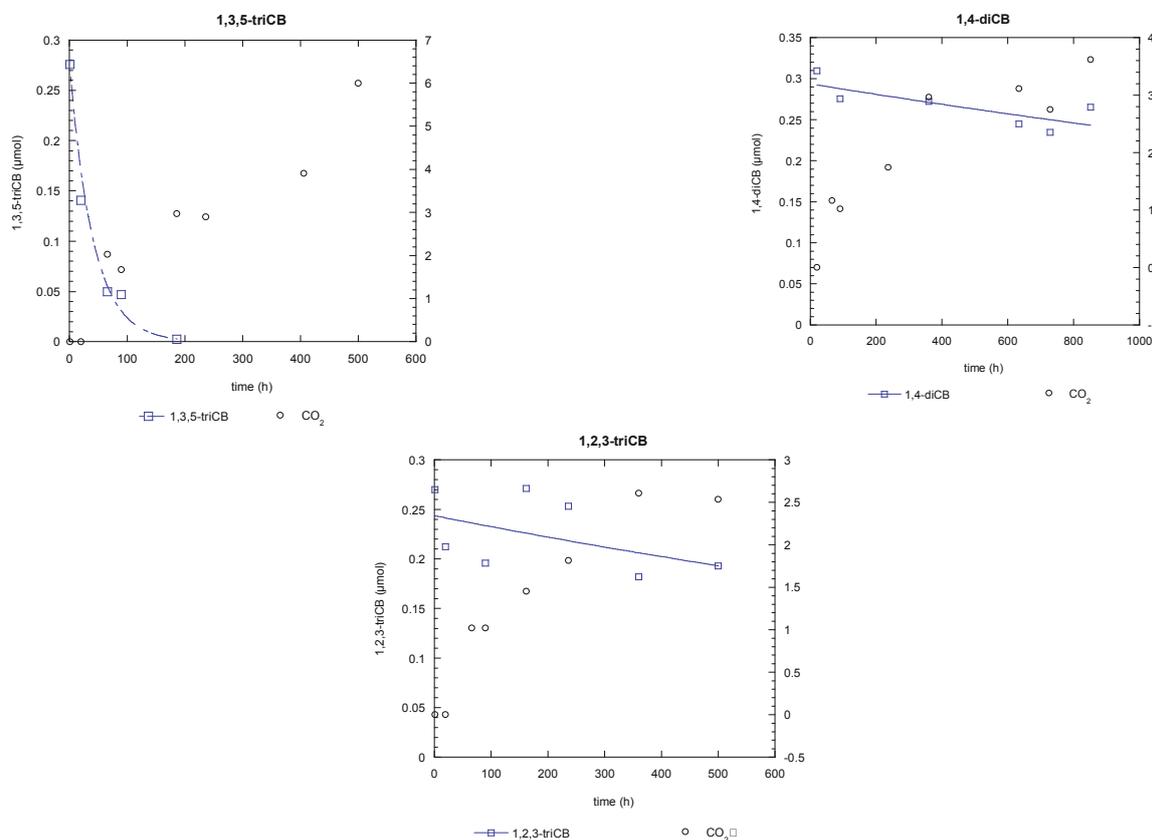
Fig. 8. Degradation profiles of aromatic compounds and CO_2 productions in pyrite suspension (20 m²/L), 25°C, initial oxygen in equivalent with atmosphere; a) 135-triCB; b) 14-diCB; c) 123-triCB. Stocks diluted in benzene at concentration of 10 mg/ml for all compounds were used
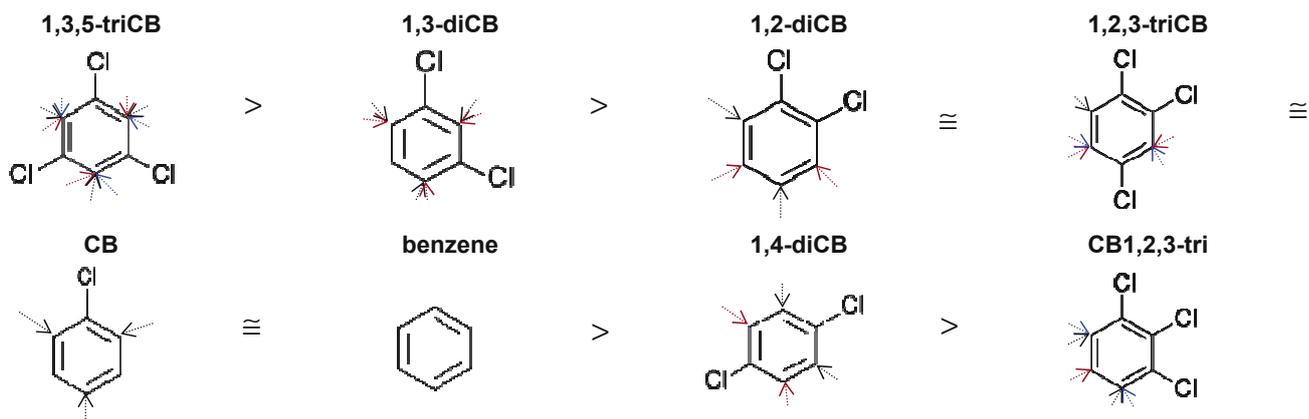
Table 2. Chloride balances of di- and tri-chlorinated benzenes in aerobic pyrite suspension (20 m^2/L)

Samples	Shaking time (h)	Cl$^-$ (µmol)	Total Cl$^-$ in degraded organics (µmol)	Cl balance (Cl$^-$/Total Cl$^-$ in degraded organics)
1,3,5-triCB	852	0.68	0.83	0.82
1,3-diCB	656	7.66	8.84	0.87
1,2-diCB	852	10.41	15.06	0.69
1,2,4-triCB	790	7.42	9.9	0.75
1,4-diCB	852	0.16	0.14	1.14
1,2,3-triCB	500	0.07	0.06	1.17

Table 3. Apparent transformation rate constants of aromatic compounds in aerobic pyrite suspension (20 m^2/L), 25°C, initial oxygen in equivalent with atmosphere

Compounds	k (h^{-1})	k (h^{-1}/m^2)
1,3,5-triCB	2.1×10-2	1.0×10-1
1,3-diCB	1.1×10-2	5.4×10-2
1,2-diCB	4.0×10-3	2.0×10-2
benzene	3.7×10-3	1.9×10-2
1,2,4-triCB	3.8×10-3	1.7×10-2
CB	3.6×10-3	1.8×10-2
1,4-diCB	1.9×10-4	9.5×10-3
1,2,3-triCB	4.2×10-5	2.1×10-4
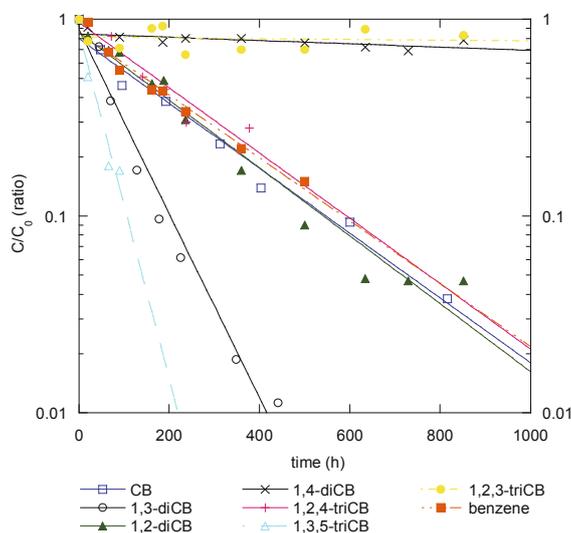
Fig. 9. Degradation profiles of mono-, di- and tri-chlorobenzenes with time in aerobic pyrite suspension (20 m^2/L), 25°C. Symbols are experimental data. Lines are the calculated curves

Oxygen consumption and pyrite oxidation products
Oxygen consumption
In the pyrite system containing oxygen and organic compounds, both pyrite and organic compounds were oxidized (directly or indirectly) following the equations (4) and (5):

$$FeS_2 + 3.5O_2 + H_2O \rightarrow Fe^{2+} + 2SO_4^{2-} + 2H^+ \qquad (4)$$

$$\text{Aromatic compounds} + O_2 \rightarrow CO_2 + (Cl^-) + H^+ \qquad (5)$$
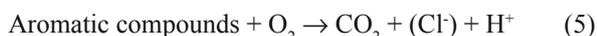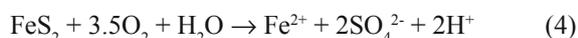
Figure 10 shows the oxygen consumption profiles with time for the experiments with and without organic compounds in aerobic pyrite suspension. Oxygen consumption profiles of the systems containing organic compounds can be divided into two groups; 1) oxygen consumed quicker than pyrite system (in the case of 1,3,5-triCB); 2) oxygen consumed less than pyrite system (in the remaining cases).

There is correlation between data for degradation profiles (Figure 9) and oxygen consumption profiles (Figure 3.10). In the case of 1,3,5-triCB, it transformed very quick, and degraded 90% after 100 h. After this period, the remaining of 1,3,5-triCB was very small. Therefore, 1,3,5-triCB was not competitive to the reactive sites on the pyrite surface. In addition, 1,3,5-triCB consumed oxygen for its degradation. Therefore, oxygen consumed was more in the presence of 1,3,5-triCB than pyrite alone. In remaining cases, the degradation rates of those organic compounds were at least 5 time smaller than of 1,3,5-triCB. Their presence at the reactive sites on the pyrite surface inhibits the oxidation reaction of pyrite at those sites. Therefore oxygen consumption was less in those systems compared to the pyrite blank system.

Pyrite oxidation products
Table 4 shows the experimental data of sulfate and ferrous ions produced in the aerobic pyrite suspension with and without organic compounds. For this data set, before measurement of sulfate and ferrous ions, all samples were kept in dark for one week. Therefore, a part of ferrous ion was precipitated as ferric hydroxide. The obtained ratio of SO_4^{2-}/Fe^{2+} was in the range of 2.35 to 3.71 which was higher than stoichiometric dissolution ratio of pyrite. However, measurements of all samples were conducted in the same condition, therefore the obtained results were comparable. Pyrite after 596h shaking released more ferrous and sulfate ions than pyrite systems containing organic compounds in a similar or longer period. Organic compounds reduced the oxidation rates of pyrite, representative by the reduction in ferrous and sulfate ion concentrations. Even in the case of 1,3,5-triCB, oxygen consumption was higher in the presence of 1,3,5-triCB (Figure 3.10), but the ferrous and sulfate were still less in the system containing organic compound. It can be again concluded that oxygen was used
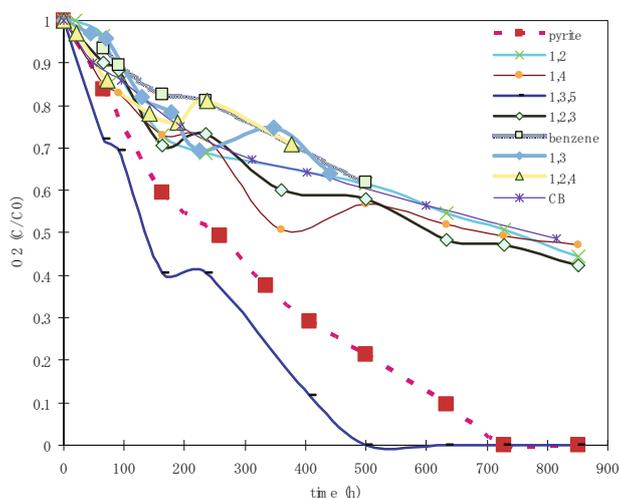
Fig. 10. Oxygen consumption profiles of and aromatic compounds (CBs or benzene) and pyrite with time under aerobic condition

Table 4. pH, Ferrous and sulfate produced in the aerobic pyrite aqueous solutions in the presence and absence of CBs or benzene

sample	time (h)	pH	Fe^{2+} (mM)	SO_4^{2-} (mM)	SO_4^{2-}/Fe^{2+}
pyrite	596	3.08	6.01	16.20	2.70
135-triCB	852	2.72	3.50	10.36	2.96
124-triCB	656	2.80	4.15	12.69	3.06
123-triCB	456	2.77	4.66	10.97	2.35
14-diCB	528	2.75	4.45	10.83	2.43
12-diCB	504	2.47	4.81	13.03	2.71
benzene	500	2.83	1.55	5.73	3.71
13-diCB	656	2.43	2.54	9.23	3.64

for both pyrite and organic compounds oxidation reactions. The presence of organic compounds reduced the oxidation rate of pyrite.

pH

The oxidation reactions of pyrite and aromatic compounds expressed in equations (4) and (5) both release protons. Table 4 compares pH of the pyrite aqueous solutions in the presence and absence of aromatic compounds. The presence of aromatic compounds reduced pH of solutions more than the system containing only pyrite after similar period. Pyrite after 596 h shaking has pH of 3.08, which is higher than pH of solutions containing organic compounds after similar or even shorter shaking period. Despite the presence of organic compounds reduced the pyrite oxidation rates, protons release was higher in the presence of organic compounds. This data means that the amount of proton released from equation (5) is larger than the amount of proton due to the reduction of pyrite oxidation.

Discussion

The results of benzene and chlorinated benzenes degradation by pyrite under aerobic condition found in this study have shownthe strong oxidation capacity of pyrite suspension in the presence of oxygen. The degradation could be due to the hydrogen peroxide and OH· induced from pyrite, which were found in our previous research (Pham et al. 2008, Pham et al. 2009) and other several researches (Ahlberg and Broo 1997, Berger et al. 1993, Borda et al. 2001, 2003, Cohn et al. 2004, 2006, 2008, Hao et al. 2006). Pyrite wasreported to be able to spontaneously form hydrogen peroxide when exposed to water (Ahlberg and Broo 1997, Borda et al. 2003, Cohn et al. 2006).

In our previous study, we were able to quantify the OH· radical generated in pyrite suspension, which increased with the increase of oxygen concentration in the reactor. Ramstidt and Vaugan (2003) proposed a Fenton-type mechanism for the reduction of O_2 generating OH· and H_2O_2 at the surface of oxidizing pyrite. This radical is the most reactive in all reactive oxygen species (ROS). In the research of Berger et al. (1993) which used purine moiety of guanine moiety of DNA as probe for the radical oxidation, pyrite was found as the most reactive mineral able to hydroxylate the guanine moiety of DNA. Cohn et al. (2004, 2006) used yeast RNA to detect the radical induced from pyrite and pyrite-containing-coal. In their research, RNA was stable in the presence of hydrogen peroxide; while it degrades in the presence of ferrous iron and hydroxyl radicals. Coal and pyrite were the most reactive both in RNA degradation and hydroxyl radical generation. Coals that contain FeS_2 generate ROS and degrade RNA. Coal samples that did not contain pyrite did not produce ROS nor degraded RNA. The concentration of generated ROS and degradation rate of RNA both increased with greater FeS_2 content in the coals.

However, the mechanism of hydroxyl radical induced from pyrite was still unclear. Borda et al (2003) proposed that the reaction between adsorbed H_2O and Fe(III), at a sulfur--deficient defect site, on the pyrite surface generates an adsorbed hydroxyl radical (OH·) following the below scheme:

$$\equiv Fe(III) + H_2O_{(ads)} \rightarrow \equiv Fe(II) + OH \cdot_{(ads)} + H^+$$
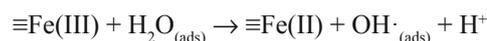
This hypothesis was not impossible, because the presence of Fe(III) on the pyrite surface and the conversion of Fe(III) to Fe(II) at the defect sites had also been reported by Nesbitt et al. (1998, 2000). The second hypothesis for hydroxyl radical induced from pyrite was that hydroxyl radical was transformed from pyrite-induced hydrogen peroxide (Cohn et al. (2006)). Another hypothesis for radical generation from pyrite was that the absorption of oxygen on the pyrite surface during pyrite oxidation induced hydroxyl radical (Ahlberg and Broo 1997, Rimstidt and Vaughan 2003). The hydroxyl radical induced from pyrite was verified and this strong radical can degrade several organic compounds. However, the mechanism as well as conditions for radical production in pyrite aqueous solution still need more clarification.

Conclusion

Pyrite can catalyze degradation of aromatic organic compounds, both chlorinated and non-chlorinated compounds. The degradation rates depend on the chemical structures; in this case it depended on the number and position of chlorine substituent on the benzene ring. The presence of organic compounds can inhibit the pyrite oxidation reactions.

References

Ahlberg, E. & Broo, A.E. (1997). Electrochemical reaction mechanisms at pyrite in acidic perchlorate solutions, *Journal of The Electrochemical Society*, 144(4), pp. 1281–1286.

ATSDR, Division of toxicology and environmental medicines. Summary data for 2007 priority list of hazardous substances.

Berger, M., De Hazen, M., Nejjari, A., Fournier, J., Gulgnard, J., Pezerat, H. & Cadet, J. (1993). Radical oxidation reaction of the purine moiety of 2′-deoxyribonucleosides and DNA by iron--containing minerals, *Carcinogenesis*, 14(1), pp. 41–46.

Borda, M.J., Elsetinow, A.R., Schoonen, M.A. & Strongin, D.R. (2001). Pyrite-induced hydrogen peroxide formation as a driving force in the evolution of photosynthetic organisms on an early Earth, *Astrobiology*, 1(3), pp. 283–288.

Borda, M.J., Elsetinow, A.R., Strongin, D.R. & Schoen, M.A. (2003). A mechanism for the production of hydroxyl radical at surface defect sites on pyrite, *Geochimica et Cosmochimica Acta*, 67(5), pp. 935–939.

Bruice, P.Y. (2004). Organic chemistry. Prentice Hall, NJ, USA.

Carlson, D.L., McGuire, M.M., Roberts, A.L. & Fairbrother, D.H. (2003). Influence of surface composition on the kinetics of alachlor reduction by iron pyrite, *Environmental Science & Technology*, 37(11), pp. 2394–2399.

Che, H. & Lee, W. (2011). Selective redox degradation of chlorinated aliphatic compounds by Fenton reaction in pyrite suspension, *Chemosphere*, 82(8), pp. 1103–1108.

Cohn, C.A., Mueller, S., Wimmer, E., Leifer, N., Greenbaum, S., Strongin, D.R. & Schoonen, M.A. (2006). Pyrite-induced hydroxyl radical formation and its effect on nucleic acids, *Geochemical Transactions*, 7(1), 3.

Cohn, C.A., Borda, M.J. & Schoonen, M.A. (2004). RNA decomposition by pyrite-induced radicals and possible role of lipids during the emergence of life, *Earth and Planetary Science Letters*, 225(3–4), pp. 271–278.

Cohn, C.A., Mueller, S., Wimmer, E., Leifer, N., Greenbaum, S., Strongin, D.R. & Schoonen, M.A. (2006). Pyrite-induced

hydroxyl radical formation and its effect on nucleic acids, *Geochemical Transactions*, 7(1), 3.

Cohn, C.A., Laffers, R. & Schoonen, M.A. (2006). Using yeast RNA as a probe for generation of hydroxyl radicals by earth materials, *Environmental Science & Technology*, 40(8), pp. 2838–2843.

Cohn, C.A., Simon, S.R. & Schoonen, M.A. (2008). Comparison of fluorescence-based techniques for the quantification of particle-induced hydroxyl radicals, Particle and Fibre Toxicology, 5, 2. doi:10.1186/1743-8977-5-2

Ennaoui, A., Fiechter S., Pettenkofer, Ch., Aloso-Vante, N., Buker, K., Bronold, M., Hopfner, Ch. & Tributsch, H. (1993). Iron sulfides for solar energy conversion, *Solar Energy Materials*, 29, pp. 289–370.

Hao, J., Cleveland, C., Lim, E., Strongin, D.R. & Schoonen, M.A. (2006). The effect of adsorbed lipid on pyrite oxidation under biotic conditions, *Geochemical Transactions*, 7(1), 8.

Hsiao, Y.L. & Nobe, K. (1993). Hydroxylation of chlorobenzene and phenol in a packed bed flow reactor with electrogenerated Fenton's reagent, *Journal of Applied Electrochemistry,* 23(9), pp. 943–946.

Kriegman-King, M.R. & Reinhard, M. (1994). Transformation of carbon tetrachloride by pyrite in aqueous solution, *Environmental Science & Technology*, 28(4), pp. 692–700.

Lee, W. & Batchelor, B. (2002). Abiotic reductive dechlorination of chlorinated ethylenes by iron-bearing soil minerals. 1. Pyrite and magnetite, *Environmental Science & Technology*, 36(23), pp. 5147–5154.

Lee, W. & Batchelor, B. (2003). Reductive capacity of natural reductants, *Environmental Science & Technology*, 37(3), pp. 535–541.

Lowson, R.T. (1982). Aqueous oxidation of pyrite by molecular oxygen, *Chemical Reviews*, 82(5), pp. 461–497.

Nefso, E.K., Burns, S.E. & McGrath, C.J. (2005). Degradation kinetics of TNT in the presence of six mineral surfaces and ferrous iron, *Journal of Hazardous Materials*, 123(1–3), pp. 79–88.

Nesbitt, H.W., Bancroft, G.M., Pratt, A.R. & Scaini, M.J. (1998). Sulfur and iron surface states on fractured pyrite surfaces, *American Mineralogist*, 83(9–10), pp. 1067–1076.

Nesbitt, H.W., Scaini, M., Hochst, H., Bancroft, G.M., Schaufuss, A.G. & Szargan, R. (2000). Synchrotron XPS evidence for Fe2+-S and Fe3+-S surface species on pyrite fracture-surfaces,

and their 3D electronic states, *American Mineralogist*, 85(5–6), pp. 850–857.

Ormad, P., Cortes, S., Puig, A. & Ovelleiro, J.L. (1997). Degradation of organochloride compounds by O_3 and $O_3H_2O_2$, *Water Research*, 31(9), pp. 2387–2391.

Plagentz, V., Ebert, M. & Dahmke, A. (2006). Remediation of ground water containing chlorinated and brominated hydrocarbons, benzene and chromate by sequential treatment using ZVI and GAC, *Environmental Geology*, 49(5), pp. 684–695.

Pham, H.T., Kitsuneduka, M., Hara, J., Suto, K. & Inoue, C. (2008). Trichloroethylene transformation by natural mineral pyrite: the deciding role of oxygen, *Environmental Science & Technology*, 42(19), pp. 7470–7475.

Pham, H.T., Suto, K. & Inoue, C. (2009). Trichloroethylene transformation in aerobic pyrite suspension: pathways and kinetic modeling, *Environmental Science & Technology*, 43(17), pp. 6744–6749.

Rimstidt, J.D. & Vaughan, D.J. (2003). Pyrite oxidation: a state-of-the-art assessment of the reaction mechanism, *Geochimica et Cosmochimica acta*, 67(5), pp. 873–880.

Sedlak, D.L. & Andren, A.W. (1991). Oxidation of chlorobenzene with Fenton's reagent, *Environmental Science & Technology*, 25(4), pp. 777–782.

Vaughan, D.J. & Lennie, A.R. (1991). The iron sulphide minerals: their chemistry and role in nature, *Science Progress*, (1933), pp. 371–388.

Weerasooriya, R. & Dharmasena, B. (2001). Pyrite-assisted degradation of trichloroethene (TCE), *Chemosphere*, 42(4), pp. 389–396.

Xu, X., Zhou, M., He, P. & Hao, Z. (2005). Catalytic reduction of chlorinated and recalcitrant compounds in contaminated water, *Journal of Hazardous Materials*, 123(1–3), pp. 89–93.

Zhang, L., Sawell, S., Moralejo, C. & Anderson, W.A. (2007). Heterogeneous photocatalytic decomposition of gas-phase chlorobenzene, *Applied Catalysis B: Environmental*, 71(3–4), pp. 135–142.

Zhu, B. W., Lim, T.T. & Feng, J. (2006). Reductive dechlorination of 1,2,4-trichlorobenzene with palladized nanoscale Fe0 particles supported on chitosan and silica, *Chemosphere*, 65(7), pp. 1137–1145.